Supporting information

Constructing Gradient Lithiophilic Structure within 3D Stable Framework for Dendrite-Free Lithium Metal Anode

Guo Cheng[a#], Youming Guo[a#], Zhouheng Jiang[a], Zixiang Shang[a], Jingjing Jiang[a*], Xueyang Li[a], Xiaoyu Wu[b*], Fang Guo[c*], Ming Chen[a,d*]

a School of Chemistry and Materials, Yangzhou University, Yangzhou 225002, Jiangsu, P. R. China

b College of Materials Science and Engineering, Linyi University, Linyi, Shandong, 276000 P. R. China

c School of Chemistry and Chemical Engineering, Yancheng Institute of Technology Yancheng 224051, Jiangsu, P. R. China

d Jiangsu Provincial Key Laboratory of Green & Functional Materials and Environmental Chemistry

# These authors contributed equally to this work

*Corresponding Authors E-mail address: jjj@yzu.edu.cn (J. Jiang); wuxiaoyu1116@163.com (X. Wu) gfycit@163.com; chenming@yzu.edu.cn (M. Chen).

1.1 Material Characterization

The microstructure, surface chemistry, and crystal structure of the electrodes were characterized using field emission scanning electron microscopy (SEM, Zeiss Sura55), X-ray photoelectron spectroscopy (XPS, ESCALAB 250Xi), and X-ray diffraction (XRD, Thermo Scientific ESCALAB 250Xi), respectively. The SEM observations were conducted at an acceleration voltage of 20 kV. The XPS analysis utilized Al Kα radiation (1486.6 eV) with a power of 180 W, while the XRD patterns were recorded using Cu Kα radiation (λ = 1.5406 Å) over a 2θ range of 10° to 80°. Constant-current charge-discharge testings were conducted on the Neware BTS-5V battery testing system. Cyclic voltammetry (CV) curves and electrochemical impedance spectroscopy (EIS) tests were performed on Chenghua-manufactured electrochemical workstation (CHI660E) from China.

1.2 DFT Theoretical Calculation Methods

All calculations were performed using spin-polarized density functional theory within the Vienna Ab Initio Simulation Package (VASP). The exchange-correlation energy was described using the generalized gradient approximation (GGA) in the Perdew-Burke-Ernzerhof (PBE) function. Projector augmented wave (PAW) potentials were employed to describe the ionic cores. A plane-wave cutoff energy of 450 eV was used in all calculations. Convergence criteria were set to 0.02 eV/Å for forces and 10^{-5} eV for electronic energy in all calculations. A 4×2×1 Monkhorst-Pack k-point mesh was used for all calculations. Gaussian smearing with a width of 0.20 eV was applied.

Van der Waals interactions were accounted for using the DFT-D3 empirical correction. A vacuum layer of 15 Å was added along the z-direction to eliminate interlayer interactions. The DFT+U method was applied with U–J values of 3.4 eV for Ni and 3.87 eV for Cu, consistent with previous reports. The definition of binding energy E_b was: $E_b = E_{Li\text{-}slab} - E_{slab} - E_{Li}$.

1.3 COMSOL multiphysics simulations

A nonlinear phase field model is established by using commercial finite element simulation software COMSOL Multiphysics 6.1, and the deposition behavior of Li^+ is studied through the secondary current module. We use the classic Kobayashi model, and the parameters are carefully selected to ensure that the simulation process is simplified and the model is as close to the real situation as possible. In the mesh setting, a Mapped mesh is generated, which reduces the roughness of dendrites. During the mesh sensitive study, the system mesh size is set as 120 ×120 with a minimum grid spacing of d_{min} =2 μm. We use an implicit time integration, with a time step of Δt = 0.2 s. The Li^+ bulk concentration is employed as c_0 =1.0 ×10^3 mol m^{-3}. The electronic conductivity of Li is 1×10^{-7} S m^{-1}. Butler-Volmer equation is applied on the Li surface to describe the Li^+ deposition process and ion flux is calculated by the Nernst-Planck formulation. For the parameter settings, the electrode length was 8 μm and the height was 6 μm. It is worth noting that the electric strength is complex model that is influenced by multiple factors. The sizes of these simulations were simplified and determined based on simultaneous consideration of model feasibility and morphometry.

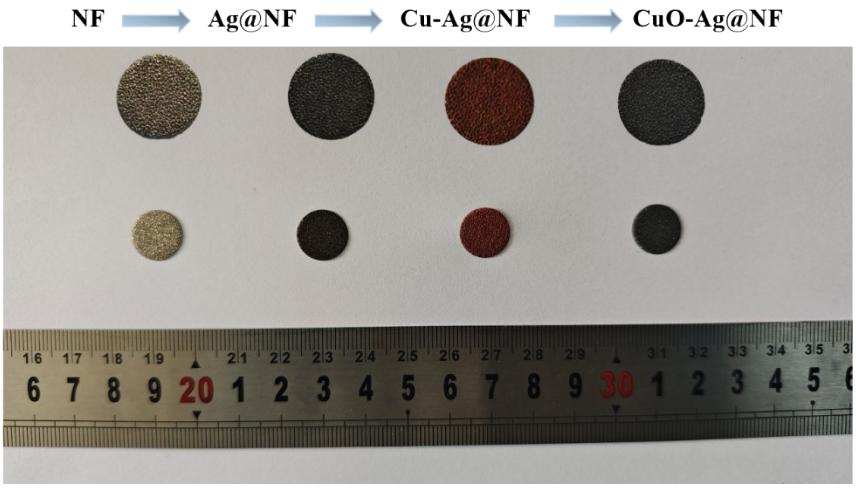

Figure S1 Optical photographs of the CuO-Ag@NF framework during the preparation process.

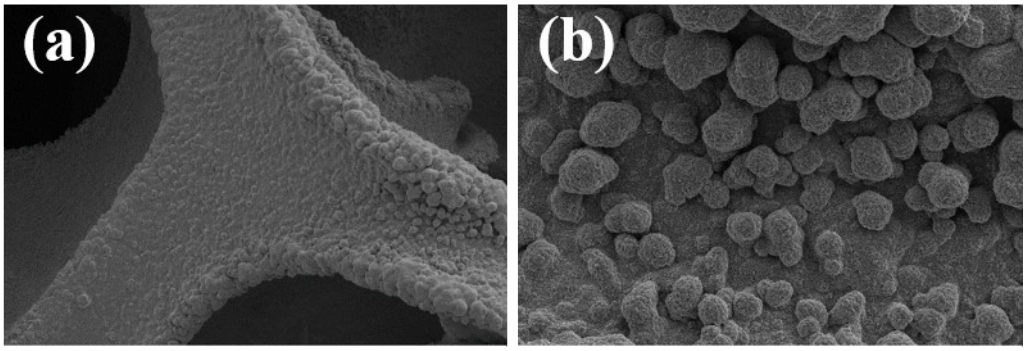

Figure S2 SEM images of CuO@NF.

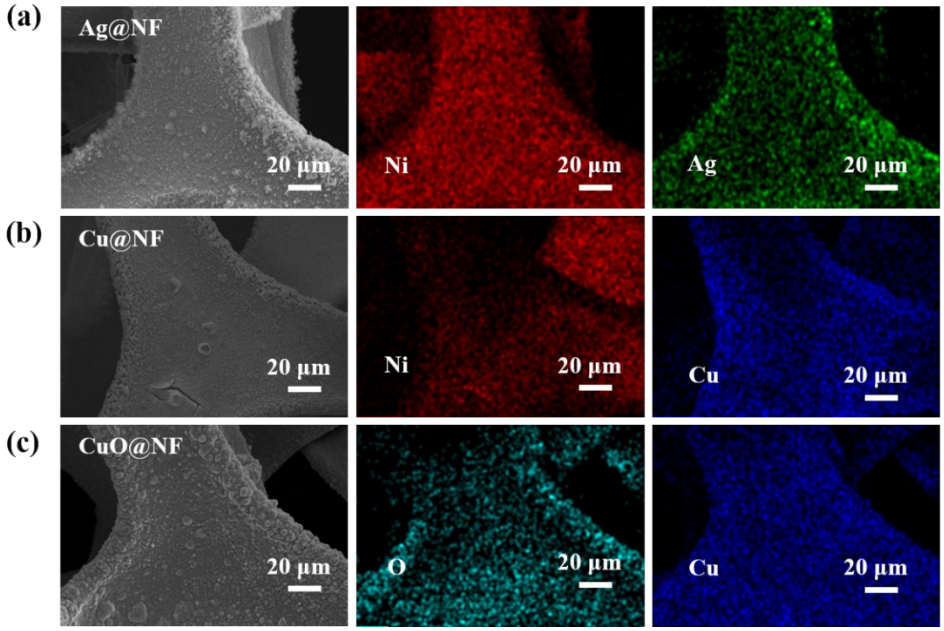

Figure S3 EDS elemental mapping: (a) Ag@NF, (b) Cu@NF, (c) CuO@NF.

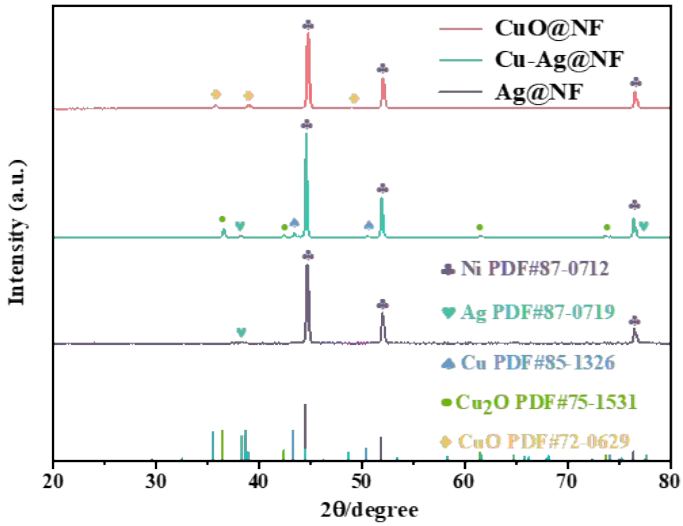

Figure S4 XRD patterns of the different frameworks.

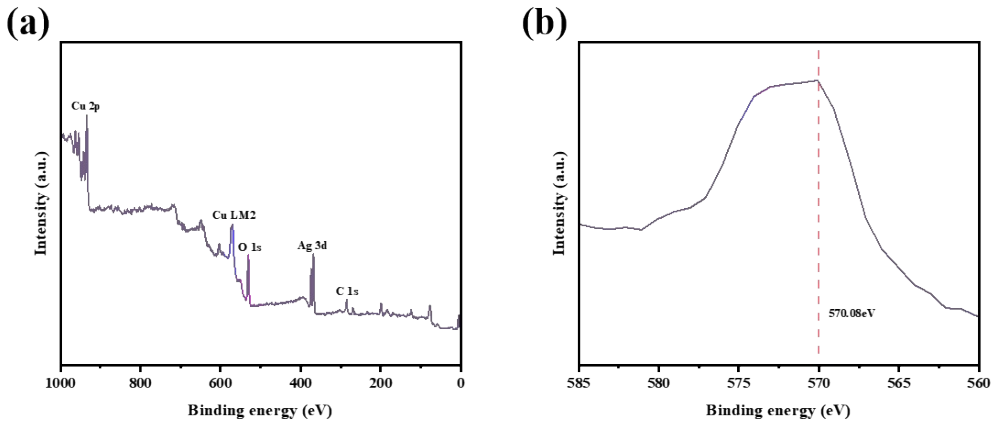

Figure S5 (a) XPS survey spectrum of CuO-Ag@NF, (b) High-resolution Cu LM2 spectrum.

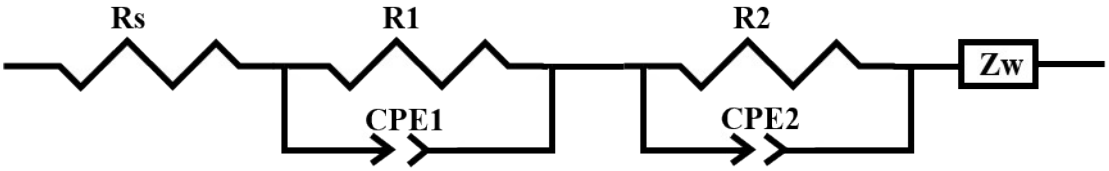

Figure S6 Equivalent circuit model for electrochemical impedance spectroscopy analysis.

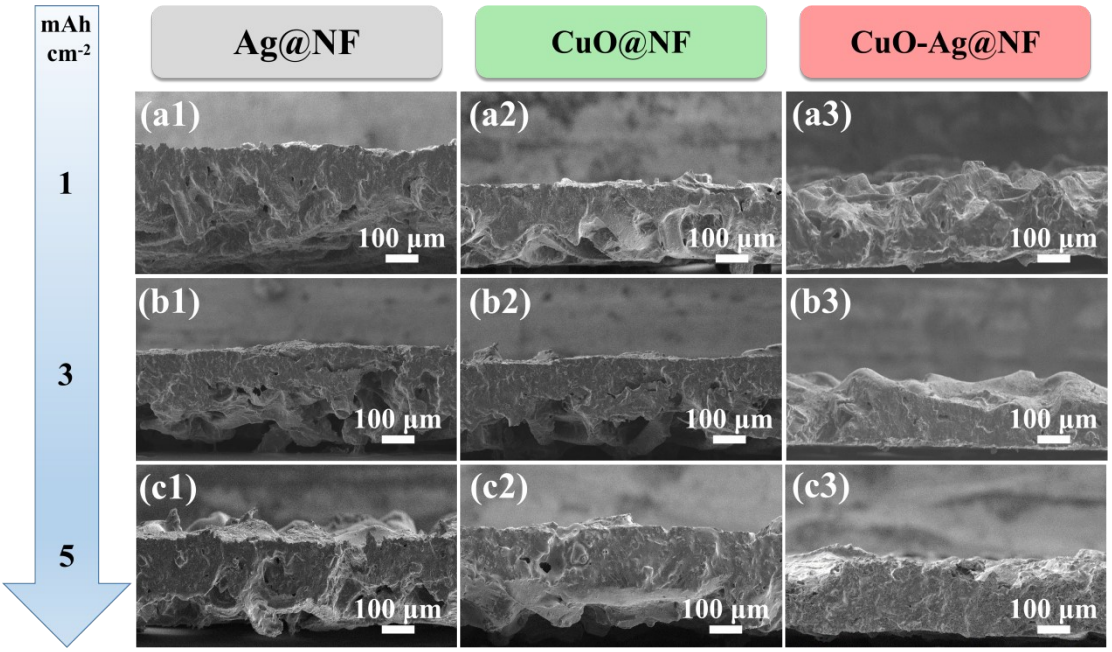

Figure S7 Morphology changes of different anodes with various Li deposition capacities at 1 mA cm^{-2} during plating/stripping. Cross-view SEM images of plating 1 mAh cm^{-2}: (a1) Ag@NF, (a2) CuO@NF, (a3) CuO-Ag@NF; plating 3 mAh cm^{-2}: (b1) Ag@NF, (b2) CuO@NF, (b3) CuO-Ag@NF; plating 5 mAh cm^{-2}: (c1) Ag@NF, (c2) CuO@NF, (c3) CuO-Ag@NF.

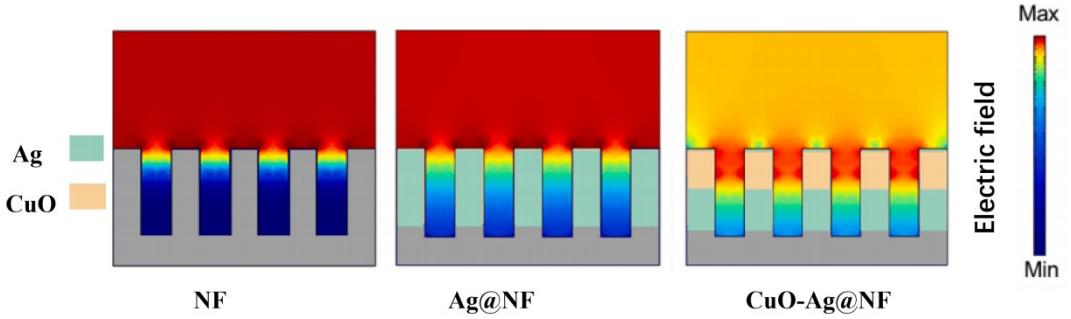

Figure S8 Finite element simulation of the electric field for Ni foam, Ag@NF, and CuO-Ag@NF after Li plating.

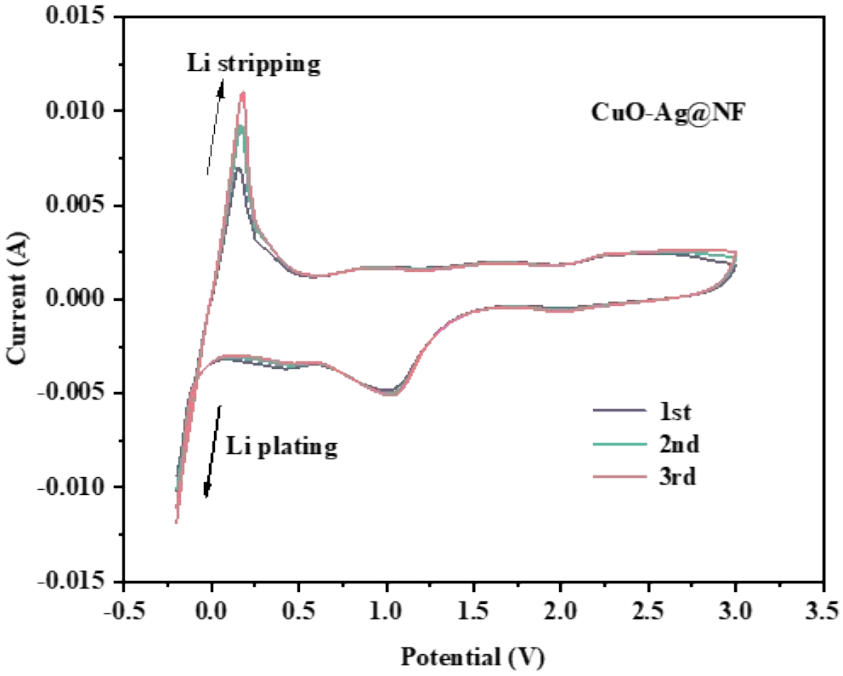

Figure S9 CV curves of CuO-Ag@NF in the half-cell configuration.

Figure S10 Optical photographs of the CuO-Ag@NF material before and after pre-lithiation.

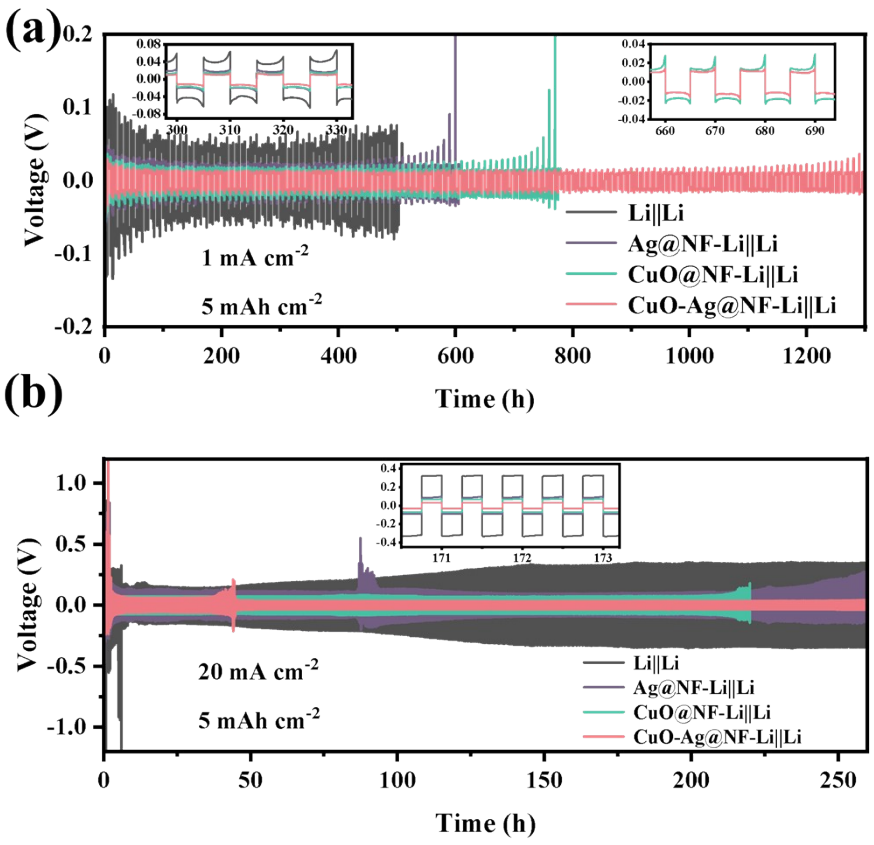

Figure S11 Voltage profiles during charging/discharging for symmetric cells with Li, Ag@NF-Li, CuO@NF-Li, and CuO-Ag@NF-Li anodes at current densities of (a) 20 mA cm^{-2} and (b) 1 mA cm^{-2} with a fixed areal capacity of 5 mAh cm^{-2}.

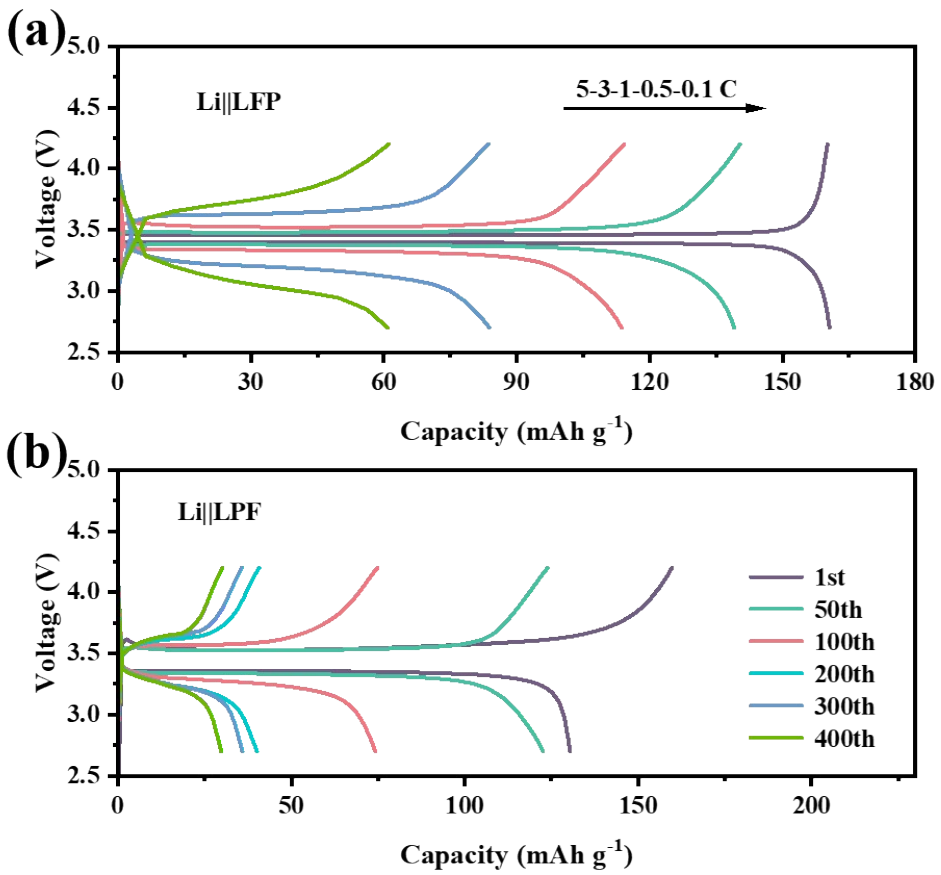

Figure S12 Charge/discharge voltage profiles of the Li||LFP full cell: (a) at varying C-rates, (b) for different cycle numbers.

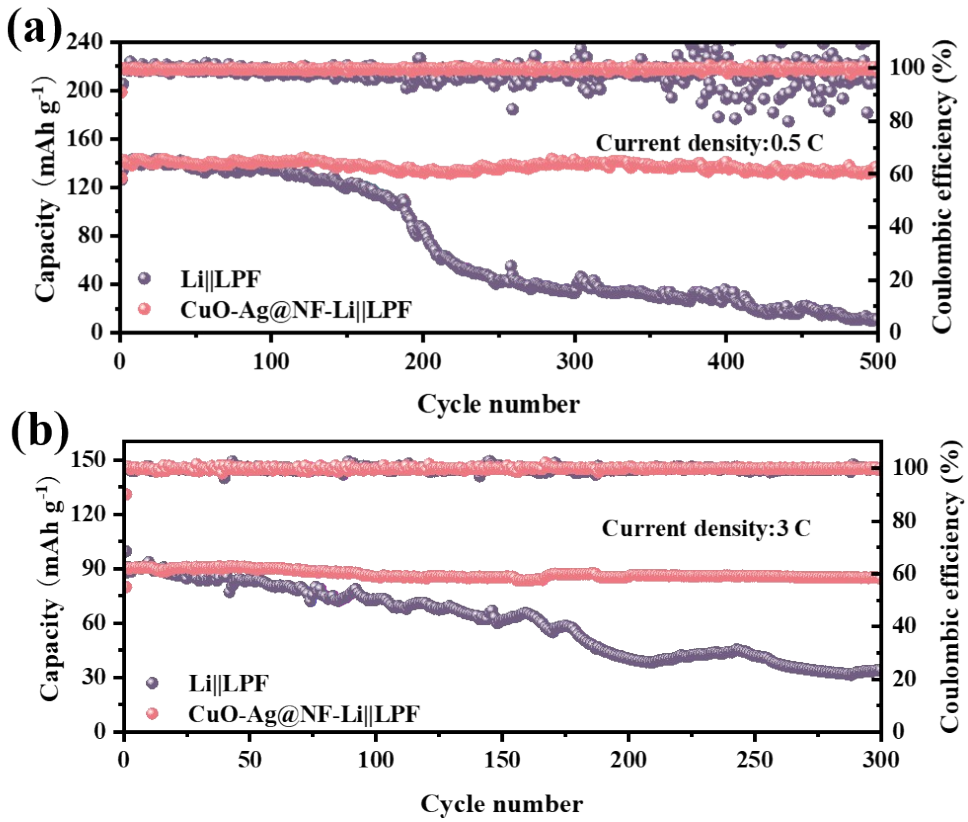

Figure S13 Long-term cycling performance of the full cell at different C-rates: (a) 0.5 C, (b) 3 C.